arXiv:hep-ph/0201132v4 8 Feb 2002

Supersymmetric Electroweak Corrections to the Higgs Boson Decays into Chargino or Neutralino Pair *

Zhang Ren-You[2], Ma Wen-Gan[1,2], Wan Lang-Hui[2], and Jiang Yi[2]
[1] CCAST (World Laboratory), P.O.Box 8730, Beijing 100080, P.R.China
[2] Department of Modern Physics, University of Science and Technology
of China (USTC), Hefei, Anhui 230027, P.R.China

Abstract

We investigate the supersymmetric electroweak corrections to the decay widths of the CP-odd and the heavy CP-even Higgs bosons into chargino or neutralino pair in the framework of the Minimal Supersymmetric Standard Model. The corrections involve the contributions of the order $O(\alpha_{ew} m_{t(b)}^3/m_W^3)$, $O(\alpha_{ew} m_{t(b)}^2/m_W^2)$ and $O(\alpha_{ew} m_{t(b)}/m_W)$. The detailed calculations of the electroweak corrections to the following decay processes: $A^0/H^0 \to \tilde{\chi}_1^+ \tilde{\chi}_1^-$ and $A^0/H^0 \to \tilde{\chi}_2^0 \tilde{\chi}_2^0$ are presented in this paper. We find that these relative corrections maybe rather large quantitatively, and can exceed 10% in some regions of parameter space. The corrections to the decay $A^0/H^0 \to \tilde{\chi}_1^0 \tilde{\chi}_2^0$ can be obtained analogously, but our results show that they are very small and can be neglected.

PACS: 12.15.Lk, 12.60.Jv, 14.80.Cp, 14.80.Ly

---

[*] Supported by National Natural Science Foundation of China.

1 Introduction

In the Standard Model (SM) [1], there exist quadratically divergent contributions to the corrections to the Higgs boson mass. This is the so-called naturalness problem of the SM. A good way to solve this problem is to consider supersymmetric (SUSY) extensions of the SM. Then the quadratic divergences can be cancelled by loop diagrams involving the supersymmetric partners of the SM particles exactly. The most attractive supersymmetric extension of the SM is the Minimal Supersymmetric Standard Model (MSSM) [2, 3]. In the MSSM, we need two Higgs doublets H_1 and H_2 to give masses to up and down type fermions and to assure the cancellation of anomalies. The Higgs spectrum consists of three neutral Higgs bosons: one CP-odd particle (A^0), two CP-even particles (h^0 and H^0), and a charged Higgs boson ($H^\pm$). At the tree level, the neutral Higgs boson masses are determined by two input parameters (see Eq.(2.13)). In this paper, we choose the mass of the CP-odd Higgs boson m_A and $\tan\beta$ as the two input parameters in Higgs sector, which is defined by $\tan\beta = v_2/v_1$, where v_1 and v_2 are the vacuum expectation values of the two Higgs boson fields H_1 and H_2, respectively. The radiative corrections to the Higgs boson masses have been discussed in Ref.[4, 5, 6]. We find that the magnitude of the corrections to m_H and m_A are less than 1% with our parameter choice, therefore they will not be considered in our calculation.

The neutral Higgs boson decays can be divided into two types of decay modes, i.e. the SM decay modes and the SUSY decay modes. The first type of decay modes (e.g. $A^0/H^0 \to \tau^+\tau^-$, $H^0 \to \gamma\gamma$ and ZZ or $ZZ^* \to 4l$) have been already carefully discussed, especially in the parameter space with large SUSY particle masses where the Higgs boson decays into sparticles are kinematically forbidden [7, 8]. But for the second type of decay modes, it has been found that the decays of the MSSM Higgs bosons into charginos or neutralinos may have substantial branching fractions when kinematically allowed, and can sometimes even dominate the usual SM decay modes [9, 10]. Moreover, the one-loop calculation of the Higgs decay into the lightest neutralino pair $(\tilde{\chi}_1^0 \tilde{\chi}_1^0)$ is important for the dark matter search[11, 12]. Therefore, the widths of these SUSY decay modes should be calculated more precisely. In this paper, we will study the radiative corrections to the decays of A^0 and H^0 into charginos or neutralinos in detail.

Considering the Yukawa corrections of the order $O(\alpha_{ew} m_{t(b)}^3/m_W^3)$, $O(\alpha_{ew} m_{t(b)}^2/m_W^2)$ and $O(\alpha_{ew} m_{t(b)}/m_W)$, we need calculate the one-loop Feynman diagrams involving the third generation of quarks and squarks which are the main contributions to the electroweak radiative corrections. The structure of this paper is as follows: in Section 2, we review briefly chargino-neutralino, squark and Higgs sectors of the MSSM, and give some results at the tree-level, in Section 3, we present our renormalization procedure, especially for the Higgs sector, and give some analytical results of the corrections to the decay widths, the numerical results and conclusions are presented in section 4, and in the Appendix, we present the explicit expressions of form factors for these decays and some necessary formulas.

2 Related theories at tree-level

2.1 Chargino and Neutralino sector

The tree-level chargino and neutralino mass matrices X, Y are [3]

$$\begin{aligned} X &= \begin{pmatrix} M & \sqrt{2} m_W \sin\beta \\ \sqrt{2} m_W \cos\beta & \mu \end{pmatrix} \\ Y &= \begin{pmatrix} M' & 0 & -m_Z s_W \cos\beta & m_Z s_W \sin\beta \\ 0 & M & m_Z c_W \cos\beta & -m_Z c_W \sin\beta \\ -m_Z s_W \cos\beta & m_Z c_W \cos\beta & 0 & -\mu \\ m_Z s_W \sin\beta & -m_Z c_W \sin\beta & -\mu & 0 \end{pmatrix} \end{aligned} \tag{2.1}$$

To obtain the tree-level masses of chargino and neutralino, we introduce three unitary matrices U, V and N to diagonalize X and Y:

$$\begin{aligned} U^* X V^{-1} &= M_D = \mathrm{diag}(m_{\tilde{\chi}_1^+}, m_{\tilde{\chi}_2^+}), \qquad (0 < m_{\tilde{\chi}_1^+} < m_{\tilde{\chi}_2^+}) \\ N^* Y N^{-1} &= N_D = \mathrm{diag}(m_{\tilde{\chi}_1^0}, m_{\tilde{\chi}_2^0}, m_{\tilde{\chi}_3^0}, m_{\tilde{\chi}_4^0}), (0 < m_{\tilde{\chi}_1^0} < m_{\tilde{\chi}_2^0} < m_{\tilde{\chi}_3^0} < m_{\tilde{\chi}_4^0}). \end{aligned} \tag{2.2}$$

where $m_{\tilde{\chi}_i^+}, (i = 1, 2)$ and $m_{\tilde{\chi}_j^0}, (j = 1, ..., 4)$ are the masses of charginos and neutralinos respectively.

2.2 Squark sector

The tree-level stop and sbottom mass matrices are

$$\begin{aligned} \mathcal{M}_{\tilde{t}}^2 &= \begin{pmatrix} M_{\tilde{Q}}^2 + m_t^2 + m_Z^2 \cos 2\beta \left(\frac{1}{2} - \frac{2}{3} s_W^2\right) & m_t \left(A_t - \mu \cot\beta\right) \\ m_t \left(A_t - \mu \cot\beta\right) & M_{\tilde{U}}^2 + m_t^2 + \frac{2}{3} m_Z^2 \cos 2\beta s_W^2 \end{pmatrix} \\ \mathcal{M}_{\tilde{b}}^2 &= \begin{pmatrix} M_{\tilde{Q}}^2 + m_b^2 - m_Z^2 \cos 2\beta \left(\frac{1}{2} - \frac{1}{3} s_W^2\right) & m_b \left(A_b - \mu \tan\beta\right) \\ m_b \left(A_b - \mu \tan\beta\right) & M_{\tilde{D}}^2 + m_b^2 - \frac{1}{3} m_Z^2 \cos 2\beta s_W^2 \end{pmatrix} \end{aligned} \tag{2.3}$$

where $M_{\tilde{Q}}, M_{\tilde{U}}, M_{\tilde{D}}$ are the soft-SUSY-breaking masses and $A_{t,b}$ the corresponding soft-SUSY-breaking trilinear coupling parameters. They can be diagonalized by unitary matrices $\mathcal{R}^{\tilde{q}}$ via

$$\mathcal{R}^{\tilde{q}} \mathcal{M}_{\tilde{q}}^2 \mathcal{R}^{\tilde{q}\dagger} = \mathrm{diag}(m_{\tilde{q}_1}^2, m_{\tilde{q}_2}^2) \tag{2.4}$$

where

$$\mathcal{R}^{\tilde{q}} = \begin{pmatrix} \cos\theta_q & \sin\theta_q \\ -\sin\theta_q & \cos\theta_q \end{pmatrix} \qquad (-\pi/2 \le \theta_{\tilde{q}} \le \pi/2, \qquad q = t, b). \tag{2.5}$$

2.3 Higgs sector

For the convenience of the Higgs potential, we introduce two $SU(2)$ Higgs doublets H_L, H_R defined as

$$H_2 = H_L, \qquad\qquad H_1 = H_R^c = i\tau_2 H_R^* \tag{2.6}$$

where τ_2 is the second Pauli matrix. The Higgs potential can be divided into four parts

$$V_H = V_H^{(1)} + V_H^{(2)} + V_H^{(3)} + V_H^{(4)} \tag{2.7}$$

which represent the linear, quadratic, cube and quartic terms respectively. In terms of the shifted fields by [5] [8]

$$H_L = \begin{pmatrix} H_{L+} \\ v_L/\sqrt{2} + H_{L0}^R + iH_{L0}^I \end{pmatrix}, \qquad H_R = \begin{pmatrix} H_{R+} \\ v_R/\sqrt{2} + H_{R0}^R + iH_{R0}^I \end{pmatrix} \tag{2.8}$$

the linear term can be expressed as

$$\begin{aligned} V_H^{(1)} &= \sqrt{2} v_L H_{L0}^R \left[m_{LH}^2 + \mid \mu \mid^2 + \frac{g^2 + g'^2}{8}(v_L^2 - v_R^2) - m^2 \frac{v_R}{v_L} \right] \\ &+ \sqrt{2} v_R H_{R0}^R \left[m_{RH}^2 + \mid \mu \mid^2 + \frac{g^2 + g'^2}{8}(v_R^2 - v_L^2) - m^2 \frac{v_L}{v_R} \right] \end{aligned} \tag{2.9}$$

where m_{LH}, m_{RH} and m are the soft-SUSY-breaking Higgs sector mass parameters. We define the coefficients of V_{L0}^R and V_{R0}^R in Eq.(2.9) to be

$$\begin{aligned} T_L &= v_L \left[m_{LH}^2 + \mid \mu \mid^2 + \frac{g^2 + g'^2}{8}(v_L^2 - v_R^2) - m^2 \frac{v_R}{v_L} \right] \\ T_R &= v_R \left[m_{RH}^2 + \mid \mu \mid^2 + \frac{g^2 + g'^2}{8}(v_R^2 - v_L^2) - m^2 \frac{v_L}{v_R} \right] \end{aligned} \tag{2.10}$$

Then the linear term of Higgs potential can be written as

$$V_H^{(1)} = \sqrt{2} H_{L0}^R T_L + \sqrt{2} H_{R0}^R T_R. \tag{2.11}$$

The quadratic Higgs potential $V_H^{(2)}$ in Eq.(2.7) consists of two parts which are relevant to charged Higgs and neutral Higgs bosons, respectively. In this paper, we only consider the radiative corrections to the MSSM neutral Higgs boson decays. The neutral Higgs part of $V_H^{(2)}$ can be written in the form [8]

$$\begin{aligned} V_H^{(2)\mathrm{neu}} = & \left(H_{L0}^I H_{R0}^I \right) \begin{pmatrix} \frac{T_L}{v_L} + m^2 \frac{v_R}{v_L} & -m^2 \\ -m^2 & \frac{T_R}{v_R} + m^2 \frac{v_L}{v_R} \end{pmatrix} \begin{pmatrix} H_{L0}^I \\ H_{R0}^I \end{pmatrix} \\ & + \left(H_{L0}^R H_{R0}^R \right) \begin{pmatrix} \frac{T_L}{v_L} + m^2 \frac{v_R}{v_L} + \frac{g^2+g'^2}{4} v_L^2 & -m^2 - \frac{g^2+g'^2}{4} v_L v_R \\ -m^2 - \frac{g^2+g'^2}{4} v_L v_R & \frac{T_R}{v_R} + m^2 \frac{v_L}{v_R} + \frac{g^2+g'^2}{4} v_R^2 \end{pmatrix} \begin{pmatrix} H_{L0}^R \\ H_{R0}^R \end{pmatrix}. \end{aligned}$$

By defining

$$\begin{aligned} \sqrt{2} \begin{pmatrix} H_{L0}^I \\ H_{R0}^I \end{pmatrix} &= S(\beta) \begin{pmatrix} G^0 \\ -A^0 \end{pmatrix} = \begin{pmatrix} \sin\beta & -\cos\beta \\ \cos\beta & \sin\beta \end{pmatrix} \begin{pmatrix} G^0 \\ -A^0 \end{pmatrix} \\ \sqrt{2} \begin{pmatrix} H_{L0}^R \\ H_{R0}^R \end{pmatrix} &= S(\alpha) \begin{pmatrix} H^0 \\ -h^0 \end{pmatrix} = \begin{pmatrix} \sin\alpha & -\cos\alpha \\ \cos\alpha & \sin\alpha \end{pmatrix} \begin{pmatrix} H^0 \\ -h^0 \end{pmatrix} \end{aligned} \tag{2.12}$$

$$\begin{aligned} & \tan\beta = \frac{v_L}{v_R}, \qquad \tan 2\alpha = \frac{m_A^2 + m_Z^2}{m_A^2 - m_Z^2} \tan 2\beta \\ & m_A^2 = m^2 \frac{v_L^2 + v_R^2}{v_L v_R} = \frac{m^2}{\sin\beta\cos\beta} \\ & m_{H,h}^2 = \frac{1}{2} \left(m_A^2 + m_Z^2 \pm \sqrt{(m_A^2 + m_Z^2)^2 - 4 m_Z^2 m_A^2 \cos^2(2\beta)} \right) \end{aligned} \tag{2.13}$$

$$\begin{aligned} T_H &= T_L \sin\alpha + T_R \cos\alpha \\ T_h &= T_L \cos\alpha - T_R \sin\alpha, \end{aligned} \tag{2.14}$$

we can get

$$\begin{aligned}
V_H^{(1)} &= T_H H^0 + T_h h^0 \\
V_H^{(2)\mathrm{neu}} &= \frac{1}{2}\left(H^0 h^0 \right)\begin{pmatrix} m_H^2 + b_{HH} & b_{Hh} \\ b_{Hh} & m_h^2 + b_{hh} \end{pmatrix}\begin{pmatrix} H^0 \\ h^0 \end{pmatrix} \\
&+ \frac{1}{2}\left(G^0 A^0 \right)\begin{pmatrix} b_{GG} & b_{GA} \\ b_{GA} & m_A^2 + b_{AA} \end{pmatrix}\begin{pmatrix} G^0 \\ A^0 \end{pmatrix} \qquad (2.15)
\end{aligned}$$

with

$$\begin{aligned}
b_{HH} &= \frac{g}{m_W \sin 2\beta}[T_H(\cos^3\alpha \sin\beta + \sin^3\alpha\cos\beta) + T_h \sin\alpha\cos\alpha\sin(\alpha-\beta)] \\
b_{hh} &= \frac{g}{m_W \sin 2\beta}[T_H \sin\alpha\cos\alpha\cos(\alpha-\beta) + T_h(\cos^3\alpha\cos\beta - \sin^3\alpha\sin\beta)] \\
b_{Hh} &= \frac{g\sin 2\alpha}{2m_W \sin 2\beta}[T_H \sin(\alpha-\beta) + T_h\cos(\alpha-\beta)] \\
b_{GG} &= \frac{g}{2m_W}[T_H\cos(\alpha-\beta) - T_h\sin(\alpha-\beta)] \\
b_{AA} &= \frac{g}{m_W \sin 2\beta}[T_H(\sin^3\beta\cos\alpha + \cos^3\beta\sin\alpha) + T_h(\cos^3\beta\cos\alpha - \sin^3\beta\sin\alpha)] \\
b_{GA} &= \frac{g}{2m_W}[T_H\sin(\alpha-\beta) + T_h\cos(\alpha-\beta)] \qquad (2.16)
\end{aligned}$$

2.4 Tree-level results

The relevant part of the MSSM Lagrangian at the tree-level to the decays concerned in this paper, can be expressed as

$$\begin{aligned}
\mathcal{L} &= \sum_{i,j=1}^{2}[-gH^0\bar{\tilde{\chi}}_i^+(P_L J_{ji}^{H*} + P_R J_{ij}^{H})\tilde{\chi}_j^+ - gh^0\bar{\tilde{\chi}}_i^+(P_L J_{ji}^{h*} + P_R J_{ij}^{h})\tilde{\chi}_j^+ \\
&+ igG^0\bar{\tilde{\chi}}_i^+(P_L J_{ji}^{G*} - P_R J_{ij}^{G})\tilde{\chi}_j^+ + igA^0\bar{\tilde{\chi}}_i^+(P_L J_{ji}^{A*} - P_R J_{ij}^{A})\tilde{\chi}_j^+] \\
&+ \frac{1}{2}\sum_{i,j=1}^{4}[gH^0\bar{\tilde{\chi}}_i^0(P_L F_{ij}^{H*} + P_R F_{ij}^{H})\tilde{\chi}_j^0 + gh^0\bar{\tilde{\chi}}_i^0(P_L F_{ij}^{h*} + P_R F_{ij}^{h})\tilde{\chi}_j^0 \\
&- igG^0\bar{\tilde{\chi}}_i^0(P_L F_{ij}^{G*} - P_R F_{ij}^{G})\tilde{\chi}_j^0 - igA^0\bar{\tilde{\chi}}_i^0(P_L F_{ij}^{A*} - P_R F_{ij}^{A})\tilde{\chi}_j^0] \qquad (2.17)
\end{aligned}$$

where $P_{L,R} = \frac{1}{2}(1 \mp \gamma_5)$, and the matrices $J_{ij}^{H,h,G,A}$, $F_{ij}^{H,h,G,A}$ are defined in Appendix A.

By using above Lagrangian, we can easily obtain

$$\begin{aligned}
\mid \mathcal{M}_t(A^0 \to \tilde{\chi}_i^+ \tilde{\chi}_j^-) \mid^2 &= g^2 \Big[(\mid J_{ij}^A \mid^2 + \mid J_{ji}^A \mid^2) m_A^2 - (\mid J_{ij}^A m_{\tilde{\chi}_i^+} - J_{ji}^{A*} m_{\tilde{\chi}_j^+} \mid^2 \\
&\quad + \mid J_{ij}^A m_{\tilde{\chi}_j^+} - J_{ji}^{A*} m_{\tilde{\chi}_i^+} \mid^2) \Big] \\
\mid \mathcal{M}_t(H^0 \to \tilde{\chi}_i^+ \tilde{\chi}_j^-) \mid^2 &= g^2 \Big[(\mid J_{ij}^H \mid^2 + \mid J_{ji}^H \mid^2) m_H^2 - (\mid J_{ij}^H m_{\tilde{\chi}_i^+} + J_{ji}^{H*} m_{\tilde{\chi}_j^+} \mid^2 \\
&\quad + \mid J_{ij}^H m_{\tilde{\chi}_j^+} + J_{ji}^{H*} m_{\tilde{\chi}_i^+} \mid^2) \Big] \\
\mid \mathcal{M}_t(A^0 \to \tilde{\chi}_i^0 \tilde{\chi}_j^0) \mid^2 &= 2g^2 \Big[\mid F_{ij}^A \mid^2 m_A^2 - \mid F_{ij}^A m_{\tilde{\chi}_i^0} - F_{ij}^{A*} m_{\tilde{\chi}_j^0} \mid^2 \Big] \\
\mid \mathcal{M}_t(H^0 \to \tilde{\chi}_i^0 \tilde{\chi}_j^0) \mid^2 &= 2g^2 \Big[\mid F_{ij}^H \mid^2 m_H^2 - \mid F_{ij}^H m_{\tilde{\chi}_i^0} + F_{ij}^{H*} m_{\tilde{\chi}_j^0} \mid^2 \Big] \qquad (2.18)
\end{aligned}$$

The tree-level decay widths can be obtained immediately after the integration over the phase space.

3 Renormalization and radiative corrections

The Feynman diagrams involving the third generation of quarks and squarks are shown in Fig.1 (Fig.1.c and Fig.1.f). In our calculation, we use the t'Hooft gauge and adopt the dimensional reduction (DR) [13] scheme, which preserves supersymmetry at least at the one-loop level. The complete on-mass-shell scheme [14, 15, 16] is used in doing renormalization.

The relevant renormalization constants in our calculation are defined as [14]:

$$\begin{aligned}
P_L\tilde{\chi}_i^+ &\to Z_{+,ij}^{L1/2}P_L\tilde{\chi}_j^+, \qquad P_R\tilde{\chi}_i^+ \to Z_{+,ij}^{R1/2}P_R\tilde{\chi}_j^+ \\
P_L\tilde{\chi}_i^0 &\to Z_{0,ij}^{L1/2}P_L\tilde{\chi}_j^0, \qquad P_R\tilde{\chi}_i^0 \to Z_{0,ij}^{R1/2}P_R\tilde{\chi}_j^0 \qquad\qquad (Z_{0,ij}^R = Z_{0,ij}^{L*}) \\
\begin{pmatrix} G^0 \\ A^0 \end{pmatrix} &\to \begin{pmatrix} 1+\frac{1}{2}\delta Z_{GG} & \frac{1}{2}\delta Z_{GA} \\ \frac{1}{2}\delta Z_{AG} & 1+\frac{1}{2}\delta Z_{AA} \end{pmatrix} \begin{pmatrix} G^0 \\ A^0 \end{pmatrix} \\
\begin{pmatrix} H^0 \\ h^0 \end{pmatrix} &\to \begin{pmatrix} 1+\frac{1}{2}\delta Z_{HH} & \frac{1}{2}\delta Z_{Hh} \\ \frac{1}{2}\delta Z_{hH} & 1+\frac{1}{2}\delta Z_{hh} \end{pmatrix} \begin{pmatrix} H^0 \\ h^0 \end{pmatrix} \\
g &\to g+\delta g, \qquad\qquad \beta \to \beta + \delta\beta \\
m_A^2 &\to m_A^2 + \delta m_A^2, \qquad\qquad m_{Z,W}^2 \to m_{Z,W}^2 + \delta m_{Z,W}^2 \\
U &\to U+\delta U, \quad V \to V+\delta V, \quad N \to N+\delta N. \qquad (3.1)
\end{aligned}$$

All these renormalization constants can be fixed by the on-mass-shell renormalization conditions:

(1) The vacuum expectation values (VEV) of H^0 and h^0 are zero [5]:

$$\langle 0 \mid H^0 \mid 0\rangle = \langle 0 \mid h^0 \mid 0\rangle = 0 \qquad (3.2)$$

At the tree-level, this means $T_H = T_h = 0$, and therefore $b_{HH,Hh,hh,GG,GA,AA} = 0$. Then from Eq.(2.15), we can get the counterterm of $V_H^{(1)}$

$$\delta V_H^{(1)} = \delta T_H H^0 + \delta T_h h^0 \qquad (3.3)$$

When we consider the radiative corrections at one-loop level, the vacuum conditions (3.2) tell us that

$$\begin{aligned}
i\hat{\Gamma}^H &= iT^H - i\delta T_H = 0 \\
i\hat{\Gamma}^h &= iT^h - i\delta T_h = 0 \qquad (3.4)
\end{aligned}$$

where $i\hat{\Gamma}^{H,h}$ are renormalized one-point Green functions (renormalized tadpoles) of H^0 and h^0, and $iT^{H,h}, -i\delta T_{H,h}$ are the contributions from the one-loop diagrams (tadpole diagrams) and conterterm, respectively.

(2) On shell conditions for MSSM Higgs bosons [5] [8]:

Analogously, we can also get the counterterm of $V_H^{(2)\mathrm{neu}}$ from Eq.(2.15). Furthermore, all the renormalized one-particle-irreducible two-point Green functions of the MSSM neutral Higgs bosons ($i\hat{\Gamma}^{HH}, i\hat{\Gamma}^{Hh}$...) can be obtained directly. The expressions of them are given in Appendix B. In our renormalization scheme, we choose m_A, m_Z as the input parameters for Higgs sector and set m_A, m_Z to be the physical masses of A^0 and Z^0:

$$m_A = m_A^{\mathrm{phys.}} \qquad\qquad m_Z = m_Z^{\mathrm{phys.}} \tag{3.5}$$

The relevant on-shell renormalization conditions for Higgs sector are

$$\begin{aligned} &i\hat{\Gamma}^{AA}(m_A^2) = i\hat{\Gamma}^{GA}(m_A^2) = 0 &&\frac{\partial i\hat{\Gamma}^{AA}(p^2)}{\partial p^2}|_{p^2=m_A^2} = i \\ &i\hat{\Gamma}^{HH}(m_H^{\mathrm{phys.2}}) = i\hat{\Gamma}^{Hh}(m_H^{\mathrm{phys.2}}) = 0 &&\frac{\partial i\hat{\Gamma}^{HH}(p^2)}{\partial p^2}|_{p^2=m_H^{\mathrm{phys.2}}} = i \end{aligned} \tag{3.6}$$

where $m_H^{\mathrm{phys.}}$ is the physical mass of H^0. Then we obtain

$$\begin{aligned} &\delta m_A^2 = \Sigma^{AA}(m_A^2) - \delta b_{AA} \\ &m_H^{\mathrm{phys.2}} = m_H^2 + \delta m_H^2 - \Sigma^{HH}(m_H^2) + \delta b_{HH} \\ &\delta Z_{AA} = -\frac{\partial \Sigma^{AA}(p^2)}{\partial p^2}\,|_{p^2=m_A^2} \qquad \delta Z_{HH} = -\frac{\partial \Sigma^{HH}(p^2)}{\partial p^2}\,|_{p^2=m_H^2} \\ &\delta Z_{GA} = \frac{2}{m_A^2}[\delta b_{GA} - \Sigma^{GA}(m_A^2)] \\ &\delta Z_{hH} = \frac{2}{m_H^2 - m_h^2}[\delta b_{Hh} - \Sigma^{Hh}(m_H^2)] \end{aligned} \tag{3.7}$$

with the definition

$$\delta m_H^2 = \frac{\partial m_H^2}{\partial m_Z^2}\delta m_Z^2 + \frac{\partial m_H^2}{\partial m_A^2}\delta m_A^2 + \frac{\partial m_H^2}{\partial \beta}\delta\beta \tag{3.8}$$

(3) For the renormalization of the parameters β and α, we use the relation between $\delta\beta$ and δZ_{GA}

$$\delta Z_{GA} = \sin 2\beta \left[2\frac{\delta \tan\beta}{\tan\beta} + \frac{\delta v_R}{v_R} - \frac{\delta v_L}{v_L} \right]$$

and impose $\delta v_L/v_L = \delta v_R/v_R$, then we have

$$\begin{aligned} \delta\beta &= \frac{\delta Z_{GA}}{4} \\ \delta\alpha &= \sin 4\alpha \left[\frac{\delta\beta}{\sin 4\beta} + \frac{m_A^2 \delta m_Z^2 - m_Z^2 \delta m_A^2}{2(m_A^4 - m_Z^4)} \right] \end{aligned} \tag{3.9}$$

The renomalization of the rest parameters and fields can be found in Ref.[14, 17, 18, 19].

By substituting Eq.(3.1) into the Lagrangian (2.17), we can obtain the counterterms of these vertices (see Eq.(5.3) in Appendix A). Then the renormalized amplitudes can be expressed as

$$\mathcal{M}_{\rm tot} = \mathcal{M}_t + \mathcal{M}_v + \mathcal{M}_c \tag{3.10}$$

where $\mathcal{M}_c$ and $\mathcal{M}_v$ represent the counterterm and the vertex corrections respectively. The divergence in $\mathcal{M}_v$ can be cancelled by that in $\mathcal{M}_c$ exactly. It can be checked both analytically and numerically. The form factors of the renormalized amplitudes $\mathcal{M}_{\rm tot}(A^0/H^0 \to \tilde{\chi}_i^+ \tilde{\chi}_j^-)$ and $\mathcal{M}_{\rm tot}(A^0/H^0 \to \tilde{\chi}_i^0 \tilde{\chi}_j^0)$ can be written as

$$\begin{aligned} J_{ij}^{\rm (tot)A,H} &= J_{ij}^{A,H} + J_{ij}^{(v)A,H} + J_{ij}^{(c)A,H} \\ F_{ij}^{\rm (tot)A,H} &= F_{ij}^{A,H} + F_{ij}^{(v)A,H} + F_{ij}^{(c)A,H} \end{aligned} \tag{3.11}$$

where $J_{ij}^{(v)A,H}$ and $F_{ij}^{(v)A,H}$ are the terms contributed by the vertex corrections. The expressions of these form factors are listed in Appendix A. Then we can get the renormalized decay width $\Gamma_{\rm tot}$ directly. To describe the magnitude of the radiative corrections to the decay width, we define the relative correction $\delta = (\Gamma_{\rm tot} - \Gamma_{\rm tree})/\Gamma_{\rm tree}$. This quantity will be used in the next section.

4 Numerical results

In this section, we present some numerical results for the quark-squark loop corrections to the chargino and nuetralino decays of A^0 and H^0. Since we find the correction to the decay $A^0/H^0 \to \tilde{\chi}_1^0\tilde{\chi}_2^0$ is very small and can be neglected, we present the results only for the decays of $A^0/H^0 \to \tilde{\chi}_1^+\tilde{\chi}_1^-/\tilde{\chi}_2^0\tilde{\chi}_2^0$ here. In our numerical calculation, the SM parameters are taken to be $m_t = 174.3$ GeV, $m_b = 4.3$ GeV, $m_Z = 91.188$ GeV, $m_W = 80.41$ GeV and $\alpha_{EW} = 1/128$ [20]. And the other MSSM parameters are determined as follows:

(1) For the parameters $M_{\tilde{Q},\tilde{U},\tilde{D}}$ and $A_{t,b}$ in sqark mass matrices, we set $M_{\tilde{Q}} = M_{\tilde{U}} = M_{\tilde{D}} = A_t = A_b = 200$ GeV.

(2) In the calculation of the corrections to the decays $A^0/H^0 \to \tilde{\chi}_1^+\tilde{\chi}_1^-$, we choose $\tan\beta$ and the masses of the two charginos $m_{\tilde{\chi}_{1,2}^+}$ as the input parameters to determine the relevant parameters in the chargino sector. Then the parameters μ and M in the mass matrix of chargino can be extracted from these input parameters. (In this paper, we assume μ is negative.)

(3) When we calculate the corrections to the decays $A^0/H^0 \to \tilde{\chi}_2^0\tilde{\chi}_2^0$, we need four independent parameters to determine the neutralino sector. Usually these parameters are

taken as $\tan\beta, M, M'$ and μ. But in our paper, we impose the relation between M and M': $M' = (5/3)\tan^2\theta_W M$ [3] and take $\tan\beta, \mu$ and $m_{\tilde{\chi}_2^0}$ as the input parameters.

In Fig.2 and Fig.3 we plot the relative corrections δ as functions of $\tan\beta$ for A^0 and H^0 decays with $m_A = 250$ GeV and $m_H = 250$ GeV respectively. In the two figures, the solid curves represent the decays $A^0/H^0 \to \tilde{\chi}_1^+\tilde{\chi}_1^-$ with the input parameters $m_{\tilde{\chi}_1^+} = 110$ GeV, $m_{\tilde{\chi}_2^+} = 300$ GeV, and the dotted curves represent the decays $A^0/H^0 \to \tilde{\chi}_2^0\tilde{\chi}_2^0$ where we take $m_{\tilde{\chi}_2^0} = 100$ GeV, $\mu = -200$ GeV. For the chargino decay of $A^0(H^0)$ (solid curve), the relative correction δ decrease from -7.5% (-13.2%) to -4.6% (-5.1%) as the increment of $\tan\beta$ from 2 to about 7, and then increase to -14.0% (-17.8%) as $\tan\beta$ to 36. The corrections to the chargino decays of A^0 and H^0 are very sensitive to the value of $\tan\beta$ and quite similar to each other. In contrast to the chargino decays of A^0 and H^0, the correction to the neutralino decay of A^0: $A^0 \to \tilde{\chi}_2^0\tilde{\chi}_2^0$ (dotted curve in Fig.2) is insensitive to the value of $\tan\beta$. It varies only from -5.4% to -7.3% as $\tan\beta$ running from 2 to 36. For the decay $H^0 \to \tilde{\chi}_2^0\tilde{\chi}_2^0$, there are two peaks at $\tan\beta \sim 1.85$ and 30 which corresponding to the resonance effects at the positions where $m_H(250\text{GeV}) \sim 2 \times m_{\tilde{t}_1}(2 \times 124.65\text{GeV})$ and $m_H(250\text{GeV}) \sim 2 \times m_{\tilde{b}_2}(2 \times 124.07\text{GeV})$ respectively. The absence of these resonance effects on the dotted curve in Fig.2 ($A^0 \to \tilde{\chi}_2^0\tilde{\chi}_2^0$) due to the fact that the couplings $V_{A^0\tilde{t}_i^\dagger\tilde{t}_j}$ and $V_{A^0\tilde{b}_i^\dagger\tilde{b}_j}$ are zero when $i = j$ (see Eq.(5.20)).

In Fig.4 and Fig.5 we present the relative corrections as functions of m_A for the chargino and neutralino decays of A^0 respectively. Here $\tan\beta$ is set to be 4 (solid curves) and 30 (dotted curves) to make comparison. The values of the relevant input parameters are given in the figures. The peaks at $m_A \sim 348$ GeV on the solid curves ($\tan\beta = 4$) in Fig.4

and Fig.5 just reflect the resonance effect at the position $m_A \sim 2 \times m_t (2 \times 174.3$ GeV). As shown in the figures, the relative corrections are insensitive to m_A and less than -7% for almost all the values in the range of 250(220) GeV to 400 GeV except for the region around the resonance position: $m_A \sim 2 \times m_t$. As mentioned in Appendix C, this top quark resonance effect are remarkable only when $\tan\beta$ is small for the appearance of $\cot\beta$ in the coupling of the vertex $A^0 - \bar{t} - t$. Therefore, there are no apparent resonance peaks at $m_A \sim 348$ GeV on the dotted curves ($\tan\beta = 30$).

In the case of the chargino decay of A^0: $A^0 \to \tilde{\chi}_1^+ \tilde{\chi}_1^-$, for $\tan\beta = 30, m_{\tilde{\chi}_1^+} = 110$ GeV and $m_{\tilde{\chi}_2^+} = 300$ GeV (dotted curve in Fig.4), the squark masses are $m_{\tilde{t}_1} = 180.96$ GeV, $m_{\tilde{t}_2} = 322.28$ GeV, $m_{\tilde{b}_1} = 241.57$ GeV and $m_{\tilde{b}_2} = 160.71$ GeV. The first squark resonance peak should appear at $m_A \sim m_{\tilde{b}_1} + m_{\tilde{b}_2} = 402.28$ GeV which is just beyond the upper limit of m_A (400 GeV), therefore it can not be displayed completely in Fig.4. As shown in Fig.4, the relative correction to this decay varies from -10.8% to -16.3% as m_A increasing from 250 GeV to 400 GeV.

For the neutralino decay of A^0: $A^0 \to \tilde{\chi}_2^0 \tilde{\chi}_2^0$, with the input parameters $\tan\beta = 30, \mu = -200$ GeV and $m_{\tilde{\chi}_2^0} = 100$ GeV, the squark masses are $m_{\tilde{t}_1} = 179.65$ GeV, $m_{\tilde{t}_2} = 323.01$ GeV, $m_{\tilde{b}_1} = 262.28$ GeV and $m_{\tilde{b}_2} = 124.07$ GeV. The sharp peak on the dotted curve in Fig.5 is just at $m_A = m_{\tilde{b}_1} + m_{\tilde{b}_2} = 386.35$ GeV. The correction increases slowly from -6% to -8% as the mass of A^0 varying from 220 GeV to 370 GeV, and then increases rapidly as m_A to 386 GeV for the resonance effect around this position.

Analogously, the m_H dependence of the corrections to the chargino and neutralino decays of H^0 are depicted in Fig.6 and Fig.7. From Fig.6 (Fig.7) we can see that for the chargino (neutralino) decay of H^0 there are three peaks on the curves. The peak on the solid curve corresponds to the resonance effect at the position $m_H = 339.88$ (315.14) GeV $\sim 2 \times m_{\tilde{t}_1} = 2 \times 170.27$ (158.00) GeV in the case of $\tan\beta = 4$. The other two peaks on the dotted curve are just at $m_H = 321.06$ (248.09) GeV $\sim 2 \times m_{\tilde{b}_2} = 2 \times 160.71$ (124.07) GeV and $m_H = 361.05$ (359.05) GeV $\sim 2 \times m_{\tilde{t}_1} = 2 \times 180.96$ (179.65) GeV. They can also be explained by the resonance effects of the chargino (neutralino) decay of H^0 with $\tan\beta = 30$. Except for the resonance effects, the corrections are about $-5\% \sim -7\%$ and insensitive to m_H when $\tan\beta = 4$. But, for $\tan\beta = 30$, the corrections can exceed -10%, especially in the case of the chargino decay of H^0, it can reach about -17%.

The relative corrections to the chargino decays of A^0 and H^0 versus the lightest chargino mass $m_{\tilde{\chi}_1^+}$ with $\tan\beta = 4$ and 30 are given in Fig.8. The upper two curves represent the cases of $\tan\beta = 4$ and the lower two, $\tan\beta = 30$. The radiative corrections to these decay modes are all insensitive to $m_{\tilde{\chi}_1^+}$. In the case of $\tan\beta = 30$, the relative corrections are considerable. They can reach about -11.7% and -15.2% for the chargino decays of A^0 and H^0 respectively.

For the neutralino decays of A^0 and H^0, $A^0/H^0 \to \tilde{\chi}_2^0\tilde{\chi}_2^0$, we plot the relative corrections as functions of $m_{\tilde{\chi}_2^0}$ in Fig.9. The curves in this figure are quite different in shape from those in Fig.8. The corrections are sensitive to $m_{\tilde{\chi}_2^0}$, especially in the case of large $\tan\beta$. For $\tan\beta = 30$, there are two small peaks on the solid and dotted curves which are just at $m_{\tilde{\chi}_2^0} = 128$ GeV $\sim m_b + m_{\tilde{b}_2} = 4.3$ GeV + 124.07 GeV. They are the only resonance peaks which can appear in this figure as $m_{\tilde{\chi}_2^0}$ in the range of 100 to 160 GeV.

In summary, we have computed the supersymmetric electroweak corrections to the partial widths of the deacys $A^0/H^0 \to \tilde{\chi}_1^+\tilde{\chi}_1^-$ and $A^0/H^0 \to \tilde{\chi}_2^0\tilde{\chi}_2^0$ in the MSSM. Only the third generation of quarks and squarks are included in our one-loop Feynman diagrams calculation. The corrections to these decay modes are all important and can exceed -10% in some parameter space, therefore they should be taken into account in the precise experiment analysis.

After the submission of this manuscript to Physical Review D, we found similar calculations in Ref.[23] where they gave the electroweak corrections to the decays $(h^0, H^0, A^0) \to \tilde{\chi}_i^0 + \tilde{\chi}_j^0$ and $\tilde{\chi}_i^0 \to (h^0, H^0, A^0) + \tilde{\chi}_j^0, (i, j = 1, 2, 3, 4)$.

Acknowledgements: This work was supported in part by the National Natural Science Foundation of China(project Nos: 19875049, 10005009), the Doctoral Program Foundation of the Education Ministry of China, and a grant from the Ministry of Science and Technology of China.

5 Appendix

5.1 Appendix A

The matrices $J^{H,h,G,A}$ and $F^{H,h,G,A}$ are defined as follows:

$$
\begin{aligned}
\begin{pmatrix} J_{ij}^H \\ J_{ij}^h \end{pmatrix} &= \begin{pmatrix} \cos\alpha & \sin\alpha \\ -\sin\alpha & \cos\alpha \end{pmatrix} \begin{pmatrix} Q_{ij} \\ S_{ij} \end{pmatrix} \\
\begin{pmatrix} J_{ij}^G \\ J_{ij}^A \end{pmatrix} &= \begin{pmatrix} -\cos\beta & \sin\beta \\ \sin\beta & \cos\beta \end{pmatrix} \begin{pmatrix} Q_{ij} \\ S_{ij} \end{pmatrix} \\
\begin{pmatrix} F_{ij}^H \\ F_{ij}^h \end{pmatrix} &= \begin{pmatrix} -\cos\alpha & \sin\alpha \\ \sin\alpha & \cos\alpha \end{pmatrix} \begin{pmatrix} Q''_{ij} \\ S''_{ij} \end{pmatrix} \\
\begin{pmatrix} F_{ij}^G \\ F_{ij}^A \end{pmatrix} &= \begin{pmatrix} \cos\beta & \sin\beta \\ -\sin\beta & \cos\beta \end{pmatrix} \begin{pmatrix} Q''_{ij} \\ S''_{ij} \end{pmatrix}
\end{aligned}
\tag{5.1}
$$

where

$$\begin{aligned}
Q_{ij} &= \frac{1}{\sqrt{2}} V_{i1} U_{j2} \\
S_{ij} &= \frac{1}{\sqrt{2}} V_{i2} U_{j1} \qquad\qquad\qquad\qquad\qquad (i,j=1,2) \\
Q''_{ij} &= \frac{1}{2}[N_{i3}(N_{j2} - N_{j1}\tan\theta_W) + N_{j3}(N_{i2} - N_{i1}\tan\theta_W)] \\
S''_{ij} &= \frac{1}{2}[N_{i4}(N_{j2} - N_{j1}\tan\theta_W) + N_{j4}(N_{i2} - N_{i1}\tan\theta_W)] \qquad (i,j=1,...,4) \quad (5.2)
\end{aligned}$$

From these definitions, we can find that Q'', S'' and $F^{H,h,G,A}$ are symmetric matrices. The counterterms of the vertices $A^0(H^0)\bar{\tilde{\chi}}_i^+ \tilde{\chi}_j^+$ and $A^0(H^0)\bar{\tilde{\chi}}_i^0 \tilde{\chi}_j^0$ can be written in the form

$$\begin{aligned}
\delta\mathcal{L} \;\; = \;\; & -gH^0 \bar{\tilde{\chi}}_i^+ (P_L J_{ji}^{(c)H*} + P_R J_{ij}^{(c)H}) \tilde{\chi}_j^+ + igA^0 \bar{\tilde{\chi}}_i^+ (P_L J_{ji}^{(c)A*} - P_R J_{ij}^{(c)A}) \tilde{\chi}_j^+ \\
& + \frac{g}{2} H^0 \bar{\tilde{\chi}}_i^0 (P_L F_{ij}^{(c)H*} + P_R F_{ij}^{(c)H}) \tilde{\chi}_j^0 - \frac{ig}{2} A^0 \bar{\tilde{\chi}}_i^0 (P_L F_{ij}^{(c)A*} - P_R F_{ij}^{(c)A}) \tilde{\chi}_j^0 \quad (5.3)
\end{aligned}$$

where $J_{ij}^{(c)A,H}$ and $F_{ij}^{(c)A,H}$ are the form factors of the counterterms.

The expression of $J_{ij}^{(c)H}$ is

$$J_{ij}^{(c)H} = \delta J_{ij}^H + \frac{\delta g}{g} J_{ij}^H + \frac{1}{2}\delta Z_{HH} J_{ij}^H + \frac{1}{2}\delta Z_{hH} J_{ij}^h + \sum_{k=1}^{2} \left[\frac{1}{2}\delta Z_{+,kj}^R J_{ik}^H + \frac{1}{2}\delta Z_{+,ki}^{L*} J_{kj}^H \right] \quad (5.4)$$

The other three form factors $J_{ij}^{(c)A}, F_{ij}^{(c)H}$ and $F_{ij}^{(c)A}$ can be written down analogously. To express the form factors $F_{ij}^{v(A,H)}$ and $J_{ij}^{v(A,H)}$ contributed by the vertex corrections, we introduce some notations to denote the vertices which will be used

$$\begin{aligned}
& A^0 - \bar{t} - t: \quad V_{A^0\bar{t}t}\gamma^5 && A^0 - \bar{b} - b: \quad V_{A^0\bar{b}b}\gamma^5 \\
& H^0 - \bar{t} - t: \quad V_{H^0\bar{t}t} && H^0 - \bar{b} - b: \quad V_{H^0\bar{b}b} \\
& A^0(H^0) - \tilde{t}_i^\dagger - \tilde{t}_j: \quad V_{A^0(H^0)\tilde{t}_i^\dagger\tilde{t}_j} && A^0(H^0) - \tilde{b}_i^\dagger - \tilde{b}_j: \quad V_{A^0(H^0)\tilde{b}_i^\dagger\tilde{b}_j} \\
& \bar{t} - \tilde{\chi}_i^0 - \tilde{t}_j: \; V^L_{\bar{t}\tilde{\chi}_i^0\tilde{t}_j} P_L + V^R_{\bar{t}\tilde{\chi}_i^0\tilde{t}_j} P_R && \bar{b} - \tilde{\chi}_i^0 - \tilde{b}_j: \; V^L_{\bar{b}\tilde{\chi}_i^0\tilde{b}_j} P_L + V^R_{\bar{b}\tilde{\chi}_i^0\tilde{b}_j} P_R \\
& \bar{t} - \tilde{\chi}_i^+ - \tilde{b}_j: \; V^L_{\bar{t}\tilde{\chi}_i^+\tilde{b}_j} P_L + V^R_{\bar{t}\tilde{\chi}_i^+\tilde{b}_j} P_R && \bar{b} - \bar{\tilde{\chi}}_i^+ - \tilde{t}_j: \; (V^L_{\bar{b}\bar{\tilde{\chi}}_i^+\tilde{t}_j} P_L + V^R_{\bar{b}\bar{\tilde{\chi}}_i^+\tilde{t}_j} P_R)C \; (5.5)
\end{aligned}$$

For the decays $A^0/H^0 \to \tilde{\chi}_i^0\tilde{\chi}_j^0$, we define

$$\begin{aligned}
&B_0 = B_0(q) \equiv B_0(-p, m_q, m_q)\\
&C^{(1)}_{0,11,12} = C^{(1)}_{0,11,12}(i,j,q,k) \equiv C_{0,11,12}(k_i, -p, m_{\tilde{q}_k}, m_q, m_q)\\
&C^{(2)}_{0,11,12} = C^{(2)}_{0,11,12}(i,j,q,k,l) \equiv C_{0,11,12}(k_i, -p, m_q, m_{\tilde{q}_k}, m_{\tilde{q}_l})
\end{aligned} \tag{5.6}$$

$$\begin{aligned}
&F_a^{A,H(1)} = F_a^{A,H(1)}(i,j,q,k) \equiv V_{A^0,H^0\bar{q}q} V^{L*}_{\bar{q}\tilde{\chi}_i^0\tilde{q}_k} V^{L}_{\bar{q}\tilde{\chi}_j^0\tilde{q}_k}\\
&F_b^{A,H(1)} = F_b^{A,H(1)}(i,j,q,k) \equiv V_{A^0,H^0\bar{q}q} V^{L*}_{\bar{q}\tilde{\chi}_i^0\tilde{q}_k} V^{R}_{\bar{q}\tilde{\chi}_j^0\tilde{q}_k}\\
&F_c^{A,H(1)} = F_c^{A,H(1)}(i,j,q,k) \equiv V_{A^0,H^0\bar{q}q} V^{R*}_{\bar{q}\tilde{\chi}_i^0\tilde{q}_k} V^{L}_{\bar{q}\tilde{\chi}_j^0\tilde{q}_k}\\
&F_d^{A,H(1)} = F_d^{A,H(1)}(i,j,q,k) \equiv V_{A^0,H^0\bar{q}q} V^{R*}_{\bar{q}\tilde{\chi}_i^0\tilde{q}_k} V^{R}_{\bar{q}\tilde{\chi}_j^0\tilde{q}_k}
\end{aligned} \tag{5.7}$$

$$\begin{aligned}
&F_a^{A,H(2)} = F_a^{A,H(2)}(i,j,q,k,l) \equiv V_{A^0,H^0\tilde{q}_l^\dagger\tilde{q}_k} V^{L*}_{\bar{q}\tilde{\chi}_i^0\tilde{q}_k} V^{L}_{\bar{q}\tilde{\chi}_j^0\tilde{q}_l}\\
&F_b^{A,H(2)} = F_b^{A,H(2)}(i,j,q,k,l) \equiv V_{A^0,H^0\tilde{q}_l^\dagger\tilde{q}_k} V^{L*}_{\bar{q}\tilde{\chi}_i^0\tilde{q}_k} V^{R}_{\bar{q}\tilde{\chi}_j^0\tilde{q}_l}\\
&F_c^{A,H(2)} = F_c^{A,H(2)}(i,j,q,k,l) \equiv V_{A^0,H^0\tilde{q}_l^\dagger\tilde{q}_k} V^{R*}_{\bar{q}\tilde{\chi}_i^0\tilde{q}_k} V^{R}_{\bar{q}\tilde{\chi}_j^0\tilde{q}_l}
\end{aligned} \tag{5.8}$$

where $q = t$ or b, $p = k_i + k_j$, k_i and k_j are the outgoing momenta of $\tilde{\chi}_i^0$ and $\tilde{\chi}_j^0$. Then the form factors $F_{ij}^{v(A,H)}$ can be written as

$$\begin{aligned}
F_{ij}^{v(A)} &= \frac{-N_c}{16\pi^2 g} \sum_{q=t,b} \left(\Lambda_{ij}^{A(1)} + \Lambda_{ij}^{A(2)}\right) + (i \leftrightarrow j)\\
F_{ij}^{v(H)} &= \frac{-iN_c}{16\pi^2 g} \sum_{q=t,b} \left(\Lambda_{ij}^{H(1)} + \Lambda_{ij}^{H(2)}\right) + (i \leftrightarrow j)
\end{aligned} \tag{5.9}$$

where $N_c = 3$,

$$\begin{aligned}
\Lambda_{ij}^{A(1)} &= \sum_{k=1}^{2} \Big[\Big(m_q m_{\tilde{\chi}_j^0} F_a^{A(1)} + (m_q^2 - m_{\tilde{q}_k}^2) F_b^{A(1)} + m_{\tilde{\chi}_i^0} m_{\tilde{\chi}_j^0} F_c^{A(1)} + m_q m_{\tilde{\chi}_i^0} F_d^{A(1)} \Big) C_0^{(1)} \\
&\quad + \Big(m_{\tilde{\chi}_i^0} m_{\tilde{\chi}_j^0} F_c^{A(1)} - m_{\tilde{\chi}_i^0}^2 F_b^{A(1)} \Big) C_{11}^{(1)} + (m_{\tilde{\chi}_i^0}^2 - m_{\tilde{\chi}_j^0}^2) F_b^{A(1)} C_{12}^{(1)} + F_b^{A(1)} B_0 \Big] \\
\Lambda_{ij}^{A(2)} &= \sum_{k,l=1}^{2} \Big[m_q F_b^{A(2)} C_0^{(2)} - m_{\tilde{\chi}_i^0} F_c^{A(2)} C_{11}^{(2)} + \Big(m_{\tilde{\chi}_i^0} F_c^{A(2)} - m_{\tilde{\chi}_j^0} F_a^{A(2)} \Big) C_{12}^{(2)} \Big] \qquad (5.10)
\end{aligned}$$

$$\begin{aligned}
\Lambda_{ij}^{H(1)} &= \sum_{k=1}^{2} \Big[\Big(m_q m_{\tilde{\chi}_j^0} F_a^{H(1)} + (m_q^2 + m_{\tilde{q}_k}^2) F_b^{H(1)} + m_{\tilde{\chi}_i^0} m_{\tilde{\chi}_j^0} F_c^{H(1)} + m_q m_{\tilde{\chi}_i^0} F_d^{H(1)} \Big) C_0^{(1)} \\
&\quad + \Big(m_{\tilde{\chi}_i^0} m_{\tilde{\chi}_j^0} F_c^{H(1)} + m_{\tilde{\chi}_i^0}^2 F_b^{H(1)} + 2 m_q m_{\tilde{\chi}_i^0} F_d^{H(1)} \Big) C_{11}^{(1)} \\
&\quad + \Big(2 m_q m_{\tilde{\chi}_j^0} F_a^{H(1)} + (m_{\tilde{\chi}_j^0}^2 - m_{\tilde{\chi}_i^0}^2) F_b^{H(1)} - 2 m_q m_{\tilde{\chi}_i^0} F_d^{H(1)} \Big) C_{12}^{(1)} - F_b^{H(1)} B_0 \Big] \\
\Lambda_{ij}^{H(2)} &= \sum_{k,l=1}^{2} \Big[m_q F_b^{H(2)} C_0^{(2)} - m_{\tilde{\chi}_i^0} F_c^{H(2)} C_{11}^{(2)} + \Big(m_{\tilde{\chi}_i^0} F_c^{H(2)} - m_{\tilde{\chi}_j^0} F_a^{H(2)} \Big) C_{12}^{(2)} \Big] \qquad (5.11)
\end{aligned}$$

For the decays $A^0/H^0 \to \tilde{\chi}_i^+ \tilde{\chi}_j^-$, we define

$$\begin{aligned}
C'^{(1)}_{0,11,12} = C'^{(1)}_{0,11,12}(i,j,q,k) &\equiv \begin{cases} C_{0,11,12}(k_i, -p, m_{\tilde{b}_k}, m_t, m_t), & q = t \\ C_{0,11,12}(k_i, -p, m_{\tilde{t}_k}, m_b, m_b), & q = b \end{cases} \\
C'^{(2)}_{0,11,12} = C'^{(2)}_{0,11,12}(i,j,q,k,l) &\equiv \begin{cases} C_{0,11,12}(k_i, -p, m_t, m_{\tilde{b}_k}, m_{\tilde{b}_l}), & q = t \\ C_{0,11,12}(k_i, -p, m_b, m_{\tilde{t}_k}, m_{\tilde{t}_l}), & q = b \end{cases} \qquad (5.12)
\end{aligned}$$

$$\begin{aligned}
J_a^{A,H(1)} = J_a^{A,H(1)}(i,j,q,k) &\equiv \begin{cases} V_{A^0,H^0\bar{t}t} V^{L*}_{\bar{t}\tilde{\chi}_i^+\tilde{b}_k} V^{L}_{\bar{t}\tilde{\chi}_j^+\tilde{b}_k}, & q = t \\ V_{A^0,H^0\bar{b}b} V^{L*}_{\bar{b}\bar{\tilde{\chi}}_i^+\tilde{t}_k} V^{L}_{\bar{b}\bar{\tilde{\chi}}_j^+\tilde{t}_k}, & q = b \end{cases} \\
J_a^{A,H(2)} = J_a^{A,H(2)}(i,j,q,k,l) &\equiv \begin{cases} V_{A^0,H^0\tilde{b}_l^\dagger\tilde{b}_k} V^{L*}_{\bar{t}\tilde{\chi}_i^+\tilde{b}_k} V^{L}_{\bar{t}\tilde{\chi}_j^+\tilde{b}_l}, & q = t \\ V_{A^0,H^0\tilde{t}_l^\dagger\tilde{t}_k} V^{L*}_{\bar{b}\bar{\tilde{\chi}}_i^+\tilde{t}_k} V^{L}_{\bar{b}\bar{\tilde{\chi}}_j^+\tilde{t}_l}, & q = b \end{cases} \qquad (5.13)
\end{aligned}$$

where k_i and k_j are the outgoing momenta of $\tilde{\chi}_i^+$ and $\tilde{\chi}_j^-$. As in Eq.(5.7) and (5.8), the definitions of $J_{b,c,d}^{A,H(1)}$ and $J_{b,c}^{A,H(2)}$ can be obtained from the definitions of $J_a^{A,H(1)}$ and $J_a^{A,H(2)}$ only by substituting for their superscripts L, L. Then the form factors $J_{ij}^{v(A,H)}$ can be expressed as follows

$$\begin{aligned}
J_{ij}^{v(A)} &= \frac{N_c}{16\pi^2 g}\left[(\Pi_{ij}^{A(1)}+\Pi_{ij}^{A(2)})\mid_{q=t} +(\Pi_{ji}^{A(1)}+\Pi_{ji}^{A(2)})\mid_{q=b}\right] \\
J_{ij}^{v(H)} &= \frac{iN_c}{16\pi^2 g}\left[(\Pi_{ij}^{H(1)}+\Pi_{ij}^{H(2)})\mid_{q=t} +(\Pi_{ji}^{H(1)}+\Pi_{ji}^{H(2)})\mid_{q=b}\right] \qquad (5.14)
\end{aligned}$$

$$\begin{aligned}
\Pi_{ij}^{A(1)} &= \sum_{k=1}^{2}\Bigg[\left(m_q m_{\tilde{\chi}_j^+} J_a^{A(1)} + \epsilon^A J_b^{A(1)} + m_{\tilde{\chi}_i^+} m_{\tilde{\chi}_j^+} J_c^{A(1)} + m_q m_{\tilde{\chi}_i^+} J_d^{A(1)}\right) C_0^{\prime(1)} \\
&\quad + \left(m_{\tilde{\chi}_i^+} m_{\tilde{\chi}_j^+} J_c^{A(1)} - m_{\tilde{\chi}_i^+}^2 J_b^{A(1)}\right) C_{11}^{\prime(1)} + (m_{\tilde{\chi}_i^+}^2 - m_{\tilde{\chi}_j^+}^2) J_b^{A(1)} C_{12}^{\prime(1)} + J_b^{A(1)} B_0\Bigg] \\
\Pi_{ij}^{A(2)} &= \sum_{k,l=1}^{2}\left[m_q J_b^{A(2)} C_0^{\prime(2)} - m_{\tilde{\chi}_i^+} J_c^{A(2)} C_{11}^{\prime(2)} + \left(m_{\tilde{\chi}_i^+} J_c^{A(2)} - m_{\tilde{\chi}_j^+} J_a^{A(2)}\right) C_{12}^{\prime(2)}\right] \quad (5.15)
\end{aligned}$$

$$\begin{aligned}
\Pi_{ij}^{H(1)} &= \sum_{k=1}^{2}\Bigg[\left(m_q m_{\tilde{\chi}_j^+} J_a^{H(1)} + \epsilon^H J_b^{H(1)} + m_{\tilde{\chi}_i^+} m_{\tilde{\chi}_j^+} J_c^{H(1)} + m_q m_{\tilde{\chi}_i^+} J_d^{H(1)}\right) C_0^{\prime(1)} \\
&\quad + \left(m_{\tilde{\chi}_i^+}^2 J_b^{H(1)} + m_{\tilde{\chi}_i^+} m_{\tilde{\chi}_j^+} J_c^{H(1)} + 2 m_q m_{\tilde{\chi}_i^+} J_d^{H(1)}\right) C_{11}^{\prime(1)} \\
&\quad + \left(2 m_q m_{\tilde{\chi}_j^+} J_a^{H(1)} + (m_{\tilde{\chi}_j^+}^2 - m_{\tilde{\chi}_i^+}^2) J_b^{H(1)} - 2 m_q m_{\tilde{\chi}_i^+} J_d^{H(1)}\right) C_{12}^{\prime(1)} - J_b^{H(1)} B_0\Bigg] \\
\Pi_{ij}^{H(2)} &= \sum_{k,l=1}^{2}\left[m_q J_b^{H(2)} C_0^{\prime(2)} - m_{\tilde{\chi}_i^+} J_c^{H(2)} C_{11}^{\prime(2)} + \left(m_{\tilde{\chi}_i^+} J_c^{H(2)} - m_{\tilde{\chi}_j^+} J_a^{H(2)}\right) C_{12}^{\prime(2)}\right] (5.16)
\end{aligned}$$

where

$$\epsilon^{A,H} = \epsilon^{A,H}(q,k) \equiv \begin{cases} m_t^2 \mp m_{\tilde{b}_k}^2, & q = t \\ m_b^2 \mp m_{\tilde{t}_k}^2, & q = b \end{cases} \qquad (5.17)$$

In this paper, we adopt the definitions and calculation formulas of the two-point and three-point Passarino-Veltman integrals shown in Ref.[21] and [22], respectively.

5.2 Appendix B

The counterterm of the potential $V_H^{(2)\mathrm{neu}}$ is

$$\begin{aligned}
\delta V_H^{(2)\mathrm{neu}} &= \frac{1}{2}H^{02}(\delta Z_{HH}m_H^2+\delta m_H^2+\delta b_{HH})+\frac{1}{2}h^{02}(\delta Z_{hh}m_h^2+\delta m_h^2+\delta b_{hh}) \\
&+ \frac{1}{2}H^0h^0(\delta Z_{Hh}m_H^2+\delta Z_{hH}m_h^2+2\delta b_{Hh})+\frac{1}{2}G^{02}\delta b_{GG} \\
&+ \frac{1}{2}A^{02}(\delta Z_{AA}m_A^2+\delta m_A^2+\delta b_{AA})+\frac{1}{2}G^0A^0(\delta Z_{AG}m_A^2+2\delta b_{GA}) \qquad (5.18)
\end{aligned}$$

Here $\delta b_{HH}, \delta b_{hh}, ...$ are functions of δT_H and δT_h. We can get their expressions from that of $b_{HH}, b_{hh}, ...$ in Eq.(2.16) by substituting δT_H and δT_h for T_H and T_h. Then the renormalized two-point Green functions can be obtained

$$\begin{aligned}
i\hat{\Gamma}^{HH}(p^2) &= i(p^2-m_H^2)+i\Sigma^{HH}(p^2)+i[\delta Z_{HH}(p^2-m_H^2)-\delta m_H^2-\delta b_{HH}] \\
i\hat{\Gamma}^{hh}(p^2) &= i(p^2-m_h^2)+i\Sigma^{hh}(p^2)+i[\delta Z_{hh}(p^2-m_h^2)-\delta m_h^2-\delta b_{hh}] \\
i\hat{\Gamma}^{Hh}(p^2) &= i\Sigma^{Hh}(p^2)+i[\frac{1}{2}\delta Z_{Hh}(p^2-m_H^2)+\frac{1}{2}\delta Z_{hH}(p^2-m_h^2)-\delta b_{Hh}] \\
i\hat{\Gamma}^{GG}(p^2) &= ip^2+i\Sigma^{GG}(p^2)+i[\delta Z_{GG}p^2-\delta b_{GG}] \\
i\hat{\Gamma}^{AA}(p^2) &= i(p^2-m_A^2)+i\Sigma^{AA}(p^2)+i[\delta Z_{AA}(p^2-m_A^2)-\delta m_A^2-\delta b_{AA}] \\
i\hat{\Gamma}^{GA}(p^2) &= i\Sigma^{GA}(p^2)+i[\frac{1}{2}\delta Z_{GA}p^2+\frac{1}{2}\delta Z_{AG}(p^2-m_A^2)-\delta b_{GA}] \qquad (5.19)
\end{aligned}$$

where the mass parameters of the $CP-$even neutral Higgs bosons m_H and m_h are determined by m_A, m_Z and $\tan\beta$ as in Eq.(2.13).

5.3 Appendix C

Here we list some of the couplings of Higgs-quark-quark and Higgs-squark-squark vertices which were used in the analysis of the numerical results:

$$\begin{aligned}
A^0 - \bar{t} - t: &\qquad V_{A^0\bar{t}t}\gamma^5 = -\frac{gm_t\cot\beta}{2m_W}\gamma^5 \\
H^0 - \bar{t} - t: &\qquad V_{H^0\bar{t}t} = -i\frac{gm_t\sin\alpha}{2m_W\sin\beta} \\
A^0 - \tilde{t}_i^\dagger - \tilde{t}_j: &\qquad V_{A^0\tilde{t}_i^\dagger\tilde{t}_j} = -\frac{gm_t}{2m_W}(\mu + A_t\cot\beta)(\mathcal{R}^{\tilde{t}}_{i1}\mathcal{R}^{\tilde{t}}_{j2} - \mathcal{R}^{\tilde{t}}_{i2}\mathcal{R}^{\tilde{t}}_{j1}) \\
A^0 - \tilde{b}_i^\dagger - \tilde{b}_j: &\qquad V_{A^0\tilde{b}_i^\dagger\tilde{b}_j} = -\frac{gm_b}{2m_W}(\mu + A_b\tan\beta)(\mathcal{R}^{\tilde{b}}_{i1}\mathcal{R}^{\tilde{b}}_{j2} - \mathcal{R}^{\tilde{b}}_{i2}\mathcal{R}^{\tilde{b}}_{j1})
\end{aligned} \tag{5.20}$$

(1) For large $\tan\beta(\gtrsim 30)$, the coupling $V_{A^0\bar{t}t}$ is suppressed due to the factor $\cot\beta$, therefore the radiative corrections to the decays $A^0 \to \tilde{\chi}_1^+\tilde{\chi}_1^-/\tilde{\chi}_2^0\tilde{\chi}_2^0$ contributed by the diagrams involving the vertex $A^0 - \bar{t} - t$ are negligible.

(2) The couplings $V_{A^0\tilde{t}_i^\dagger\tilde{t}_j}$ and $V_{A^0\tilde{t}_i^\dagger\tilde{t}_j}$ are zero when $i = j$.

References

[1] S. Weinberg, Phys. Rev. Lett. **19** (1967) 1264; S. Glashow, Nucl. Phys. **22** (1961) 579; A. Salam, in *Elementary Particle Theory*, ed. N. Svartholm, (1968) p367.

[2] H. P. Nilles Phys. Rep. **110** (1984) 1; H. E. Haber, G. L. Kane, Phys. Rep. **117** (1985) 75.

[3] J. F. Gunion, H. E. Haber, Nucl. Phys. **B272** (1986) 1.

[4] M. S. Beger, Phys. Rev. **D41** (1990) 225; D. M. Pierce, A. Papadopolous, S. B. Johnson, Phys. Rev. Lett. **22** (1992) 3678.

[5] A. Dabelstein, Z. Phys. **C67** (1995) 495, hep-ph/9409375.

[6] H. Haber, R. Hempfling, Phys. Rev. Lett. **66** (1991) 1815; Y. Okada, M. Yamaguchi, T. Yanagida, Prog. Theor. Phys. **85** (1991) 1; J. Ellis, G. Ridolfi, F. Zwirner, Phys. Lett. **B257** (1991) 83; Phys. Lett. **B262** (1991) 477; R. Barbieri, M. Frigeni, Phys. Lett. **B258** (1991) 395; S. Heinemeyer, W. Hollik, G. Weiglein, Eur. Phys. Jour. **C9** (1999) 343.

[7] R. Kinnunen, D. Denegri, CMS Note 99-037; R. Kinnunen, CMS Note 2000-0454.

[8] D. Pierce, A. Papadopoulos, Phys. Rev. **D47** (1993) 222.

[9] H. Baer, M. Bisset, D. Dicus, C. Kao, X. Tata, Phys. Rev. **D47** (1993) 1062.

[10] A. Djouadi, Mod. Phys. Lett. **A14** (1999) 359; A. Djouadi, P. Janot, J. Kalinowski, P. M. Zerwas, Phys. Lett. **B376** (1996) 220.

[11] A.Djouadi, M. Drees, P. Fileviez Perez and M. Mühlleitner, hep-ph/0109283.

[12] M. Drees, M. M. Nojiri, D. P. Roy, Y. Yamada, Phys. Rev. **D56** (1997) 276, Erratum-ibid. **D64** (2001) 039901, hep-ph/9701219.

[13] D. M. Copper, D. R. T. Jones, P. van Nieuwennuizen, Nucl. Phys. **B167** (1980) 479; W. Siegel, Phys. Lett. **B84** (1979) 193.

[14] A. Denner, Fortschr. Phys. **41** (1993) 307.

[15] M. Böhm, H. Spiesberger, W. Hollik, Fortsch. Phys. **34** (1986) 687; W. Hollik, Fortschr. Phys. **38** (1990) 165.

[16] P. Chankowski, S. Pokorski, J. Rosiek, Nucl. Phys. **B423** (1994) 437.

[17] A. Denner, T. Sack, Nucl. Phys. **B347** 203 (1990); Y. Yamada, Phys. Rev. **D64** (2001) 036008, hep-ph/0103046.

[18] H. Eberl, M. Kincel, W. Majerotto, Y. Yamada, hep-ph/0104109.

[19] K. Aoki, Z. Hioki, R. Kawabe, M. Konuma, T. Muta, Prog. Theor. Phys. **73** Suppl. (1982) 1.

[20] Particle Data Group, Eur. Phys. J. **C15** (2000) 1.

[21] Bernd A. Kniehl, Phys. Rep. **240** (1994) 211.

[22] G. Passarino and M. Veltman, Nucl. Phys. **B160**, (1979) 151.

[23] H. Eberl, M. Kincel, W. Majerotto and Y. Yamada, hep-ph/0111303.

Figure Captions

Fig.1 The relevant Feynman diagrams to the decays $A^0/H^0 \to \tilde{\chi}_i^0\tilde{\chi}_j^0$, $A^0/H^0 \to \tilde{\chi}_i^+\tilde{\chi}_j^-$: (a) and (d) tree-level diagrams; (b) and (e) counterterms for vertices; (c-1)-(c-4) and (f-1)-(f-4) one-loop vertex corrections. In diagrams (a), (b) and (c), $i = j = 2$, (d), (e) and (f), $i = j = 1$. In all the loop diagrams, the subscripts k and l run from 1 to 2.

Fig.2 The relative correction to A^0 decay as a function of $\tan\beta$. The solid and dotted curves represent the decays $A^0 \to \tilde{\chi}_1^+\tilde{\chi}_1^-$ and $A^0 \to \tilde{\chi}_2^0\tilde{\chi}_2^0$ respectively.

Fig.3 The relative correction to H^0 decay as a function of $\tan\beta$. The solid and dotted curves represent the decays $H^0 \to \tilde{\chi}_1^+ \tilde{\chi}_1^-$ and $H^0 \to \tilde{\chi}_2^0 \tilde{\chi}_2^0$ respectively.

Fig.4 The relative correction to the decay $A^0 \to \tilde{\chi}_1^+ \tilde{\chi}_1^-$ as a function of m_A.

Fig.5 The relative correction to the decay $A^0 \to \tilde{\chi}_2^0 \tilde{\chi}_2^0$ as a function of m_A.

Fig.6 The relative correction to the decay $H^0 \to \tilde{\chi}_1^+ \tilde{\chi}_1^-$ as a function of m_H.

Fig.7 The relative correction to the decay $H^0 \to \tilde{\chi}_2^0 \tilde{\chi}_2^0$ as a function of m_H.

Fig.8 The relative correction as a function of $m_{\tilde{\chi}_1^+}$. The solid (dotted) curves represent the decay $H^0 \to \tilde{\chi}_1^+ \tilde{\chi}_1^-$ ($A^0 \to \tilde{\chi}_1^+ \tilde{\chi}_1^-$) for $\tan\beta = 4$ and 30. The input parameters are set to be $m_H = 350$ GeV ($m_A = 350$ GeV) and $m_{\tilde{\chi}_2^+} = 300$ GeV.

Fig.9 The relative correction as a function of $m_{\tilde{\chi}_2^0}$. The solid (dotted) curves represent the decay $H^0 \to \tilde{\chi}_2^0 \tilde{\chi}_2^0$ ($A^0 \to \tilde{\chi}_2^0 \tilde{\chi}_2^0$) for $\tan\beta = 4$ and 30. The input parameters are set to be $m_H = 350$ GeV ($m_A = 350$ GeV) and $\mu = -200$ GeV.

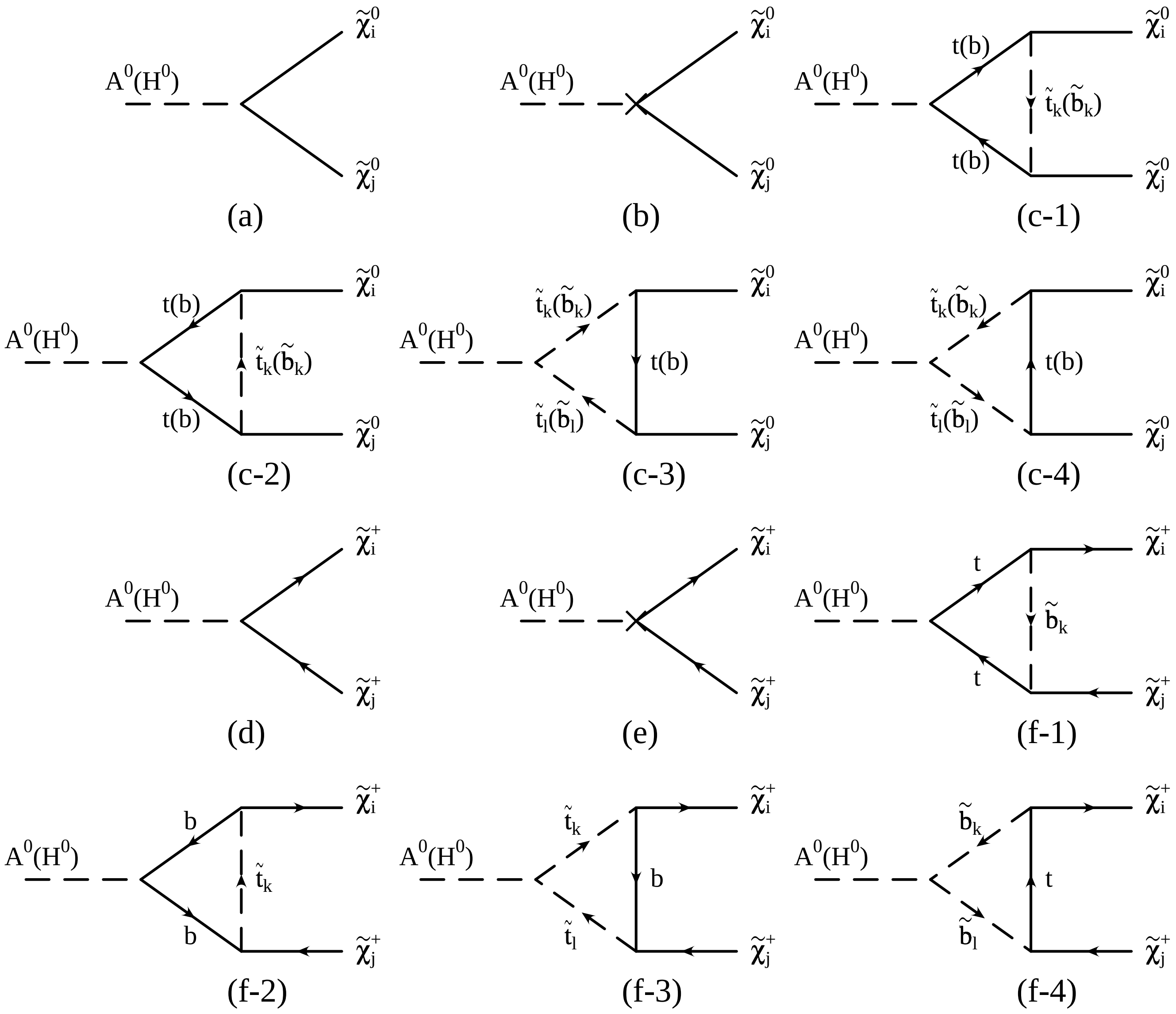
A^0(H^0)
$\tilde{\chi}_i^0$
$\tilde{\chi}_j^0$
(a)
(b)
t(b)
$\tilde{t}_k(\tilde{b}_k)$
(c-1)
(c-2)
t(b)
$\tilde{t}_l(\tilde{b}_l)$
(c-3)
(c-4)
$\tilde{\chi}_i^+$
$\tilde{\chi}_j^+$
(d)
(e)
t
$\tilde{b}_k$
(f-1)
b
$\tilde{t}_k$
(f-2)
$\tilde{t}_l$
(f-3)
$\tilde{b}_l$
(f-4)

Fig.1

Fig.2

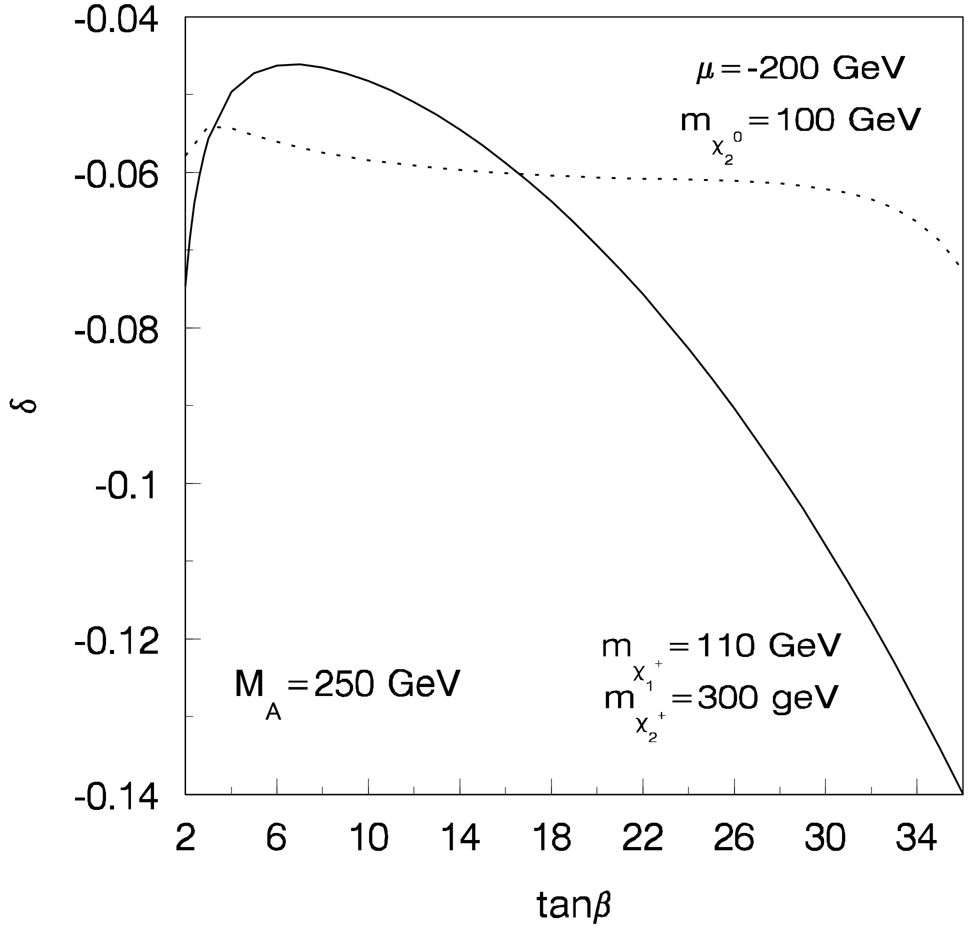

-0.04
-0.06
-0.08
-0.1
-0.12
-0.14
δ
2
6
10
14
18
22
26
30
34
$\tan\beta$
μ=-200 GeV
$m_{\chi_2^0}$=100 GeV
M_A=250 GeV
$m_{\chi_1^+}$=110 GeV
$m_{\chi_2^+}$=300 geV

Fig.3

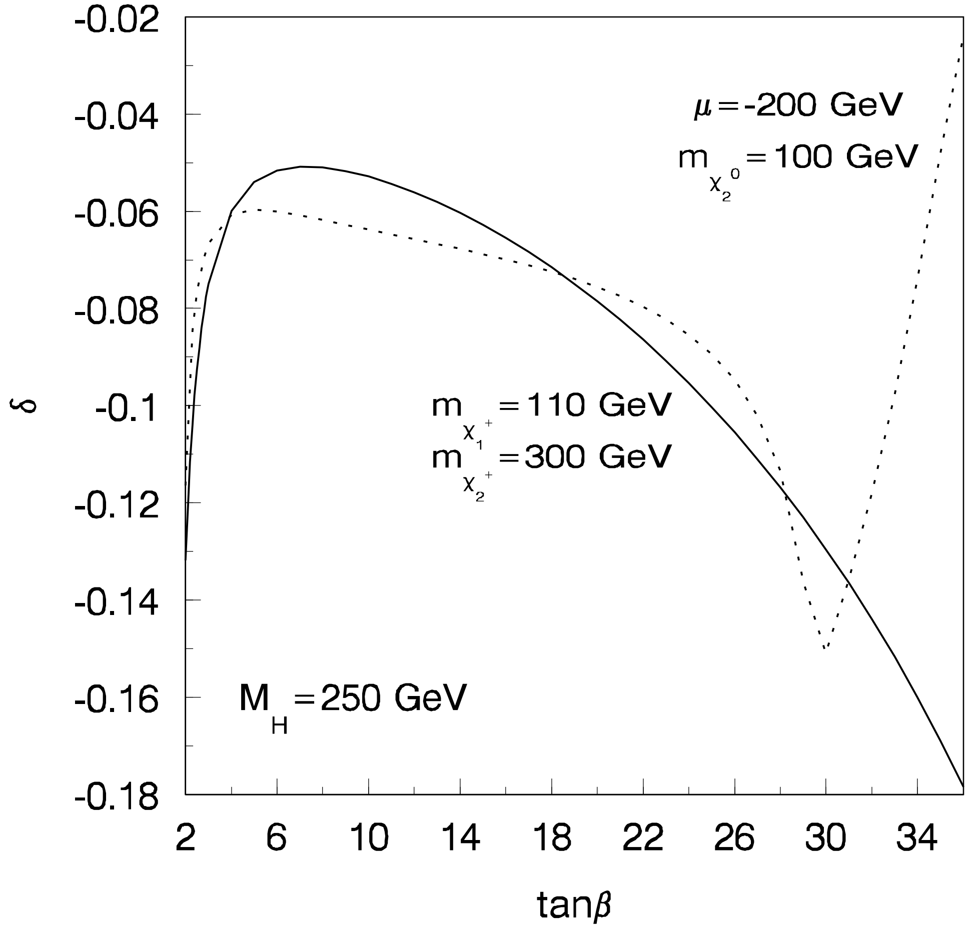

-0.02
-0.04
-0.06
-0.08
-0.1
-0.12
-0.14
-0.16
-0.18
δ
2
6
10
14
18
22
26
30
34
$\tan\beta$
$\mu = -200$ GeV
$m_{\chi_2^0} = 100$ GeV
$m_{\chi_1^+} = 110$ GeV
$m_{\chi_2^+} = 300$ GeV
$M_H = 250$ GeV

Fig.4

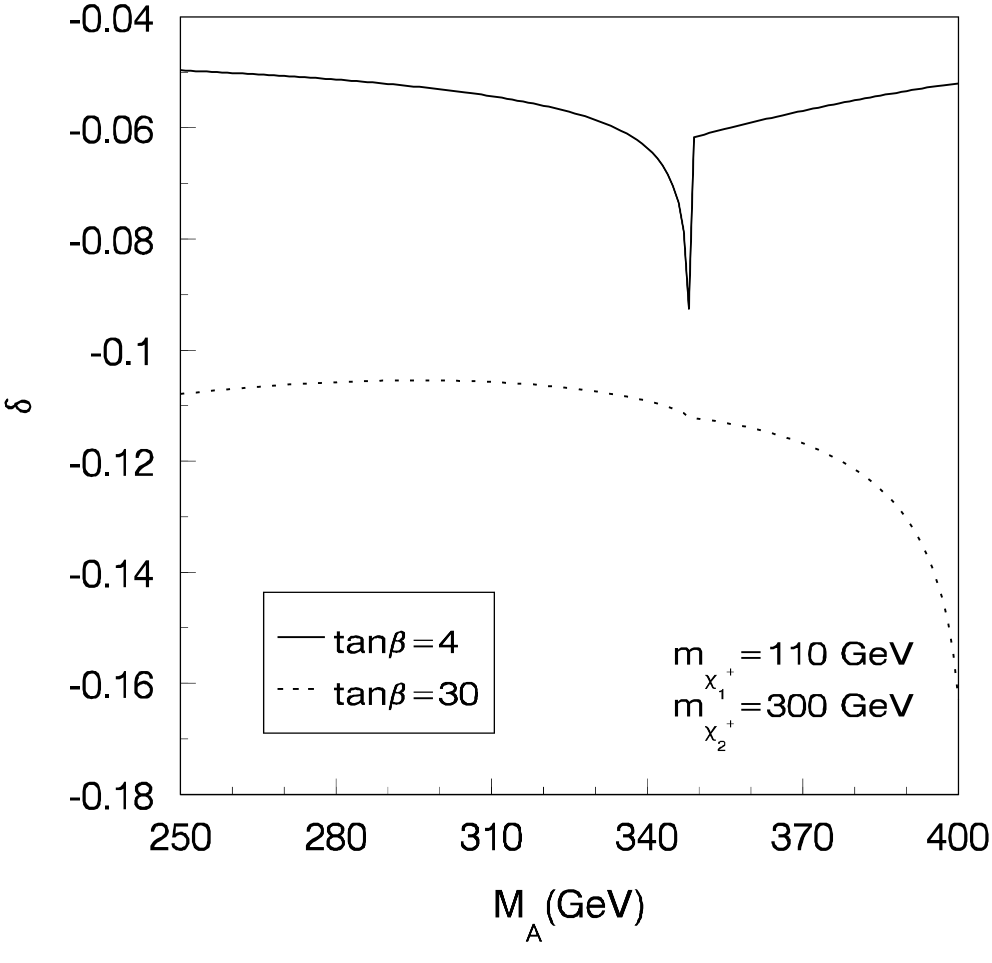

-0.04
-0.06
-0.08
-0.1
-0.12
-0.14
-0.16
-0.18
δ
250
280
310
340
370
400
M_A(GeV)
tanβ=4
tanβ=30
$m_{\chi_1^+}$=110 GeV
$m_{\chi_2^+}$=300 GeV

Fig.5

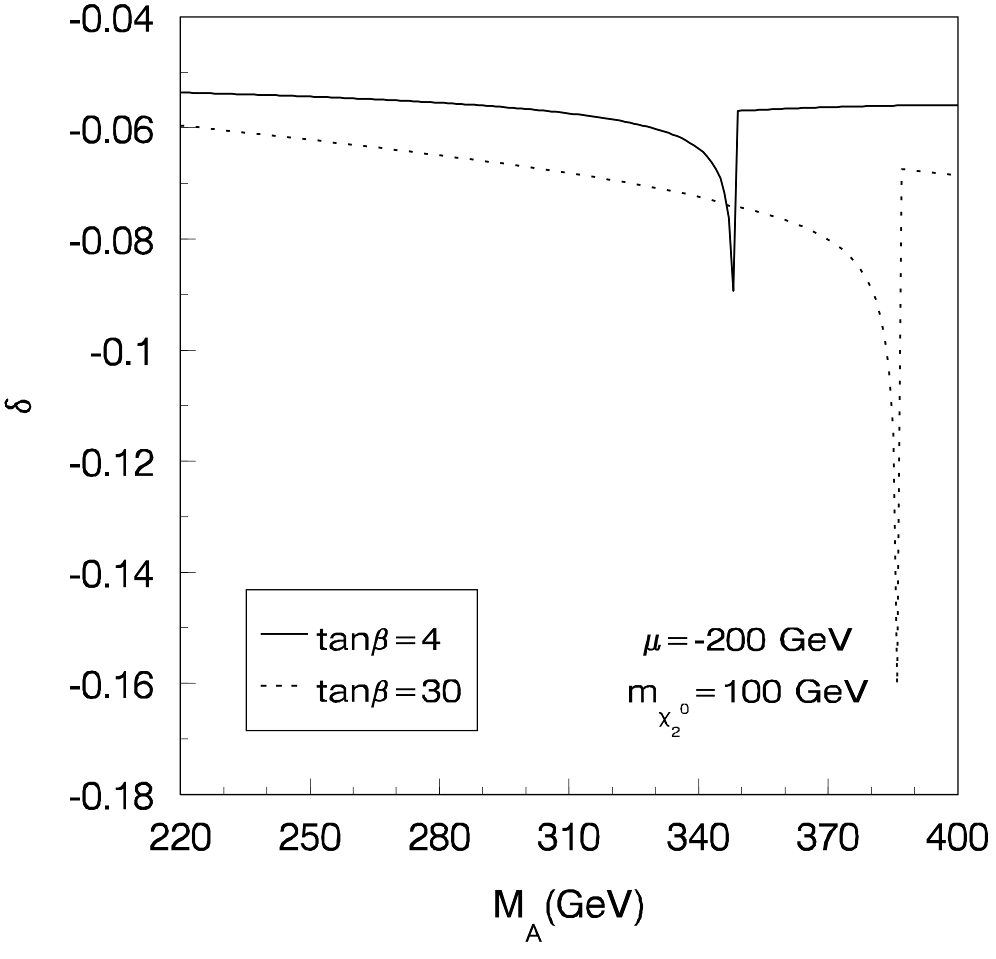

-0.04
-0.06
-0.08
-0.1
-0.12
-0.14
-0.16
-0.18
δ
220
250
280
310
340
370
400
M_A(GeV)
$\tan\beta=4$
$\tan\beta=30$
$\mu=$-200 GeV
$m_{\chi_2^0}=100$ GeV

Fig.6

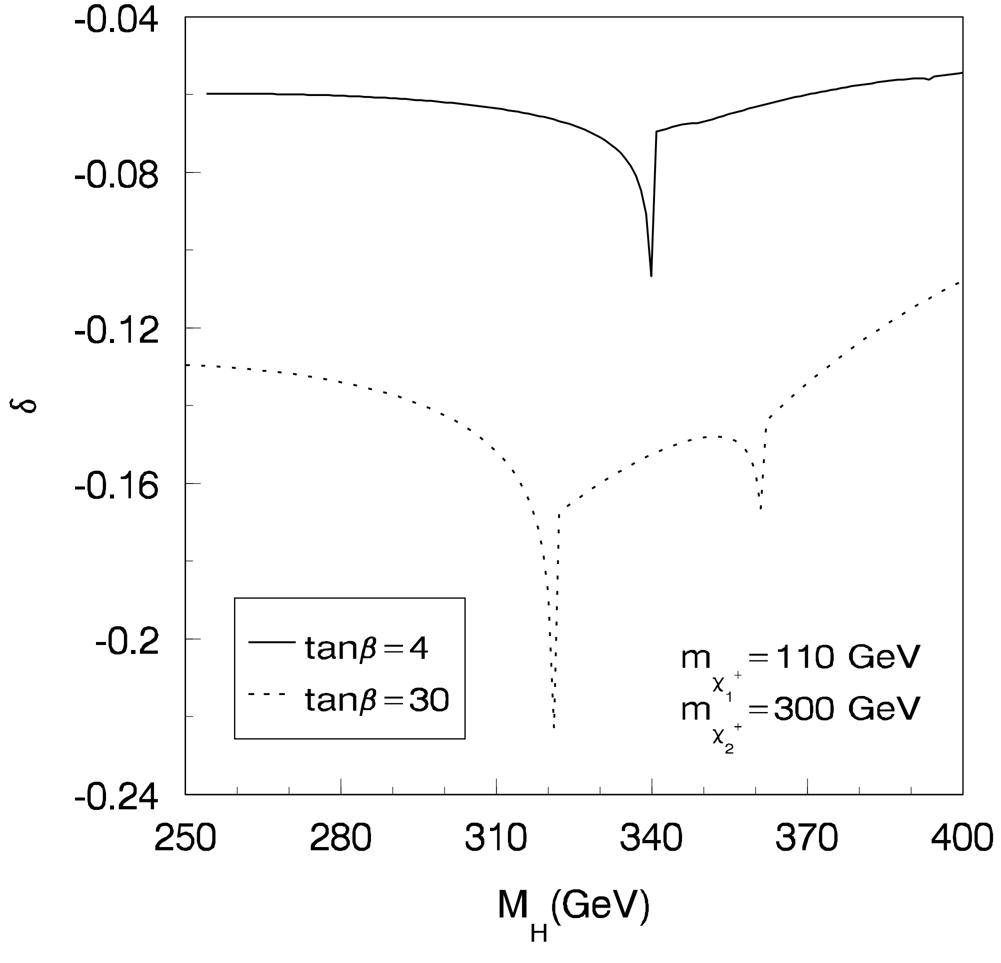
-0.04
-0.08
-0.12
-0.16
-0.2
-0.24
δ
250
280
310
340
370
400
M_H(GeV)
$\tan\beta = 4$
$\tan\beta = 30$
$m_{\chi_1^+} = 110$ GeV
$m_{\chi_2^+} = 300$ GeV

Fig.7

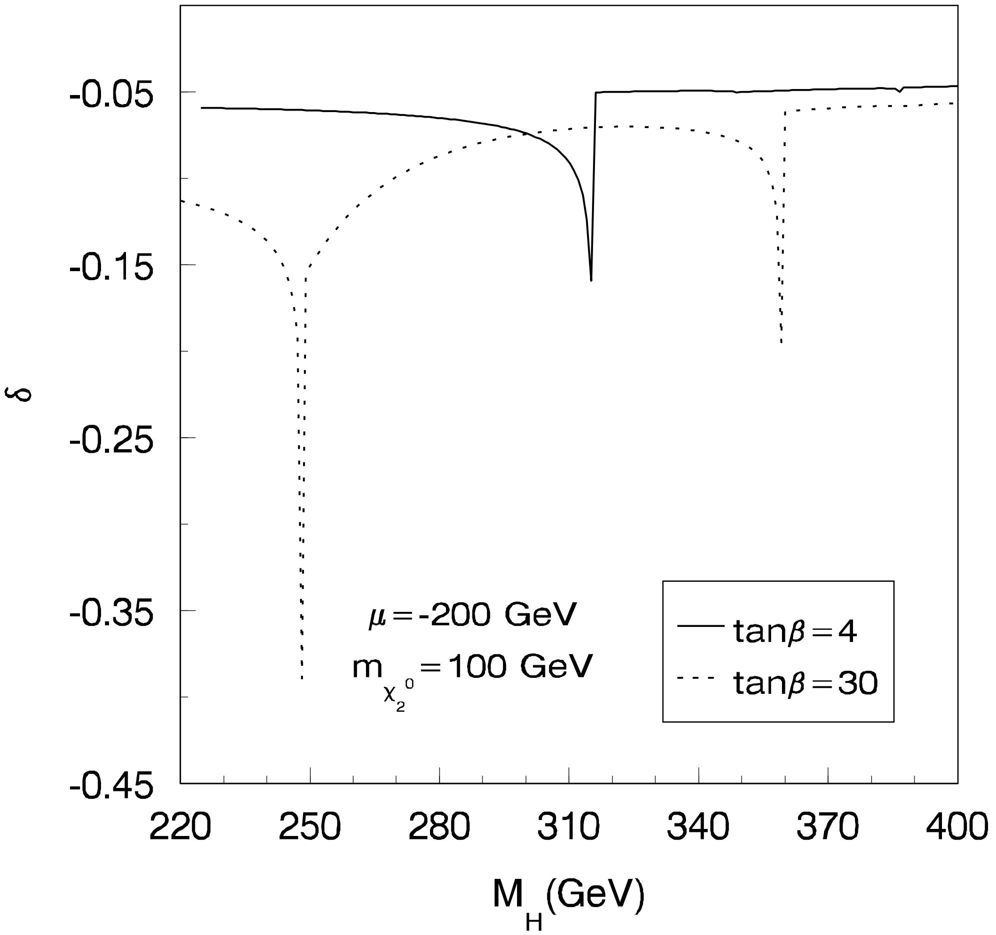

-0.05
-0.15
-0.25
-0.35
-0.45
δ
220
250
280
310
340
370
400
M_H(GeV)
μ=-200 GeV
m_χ₂⁰=100 GeV
tanβ=4
tanβ=30

Fig.8

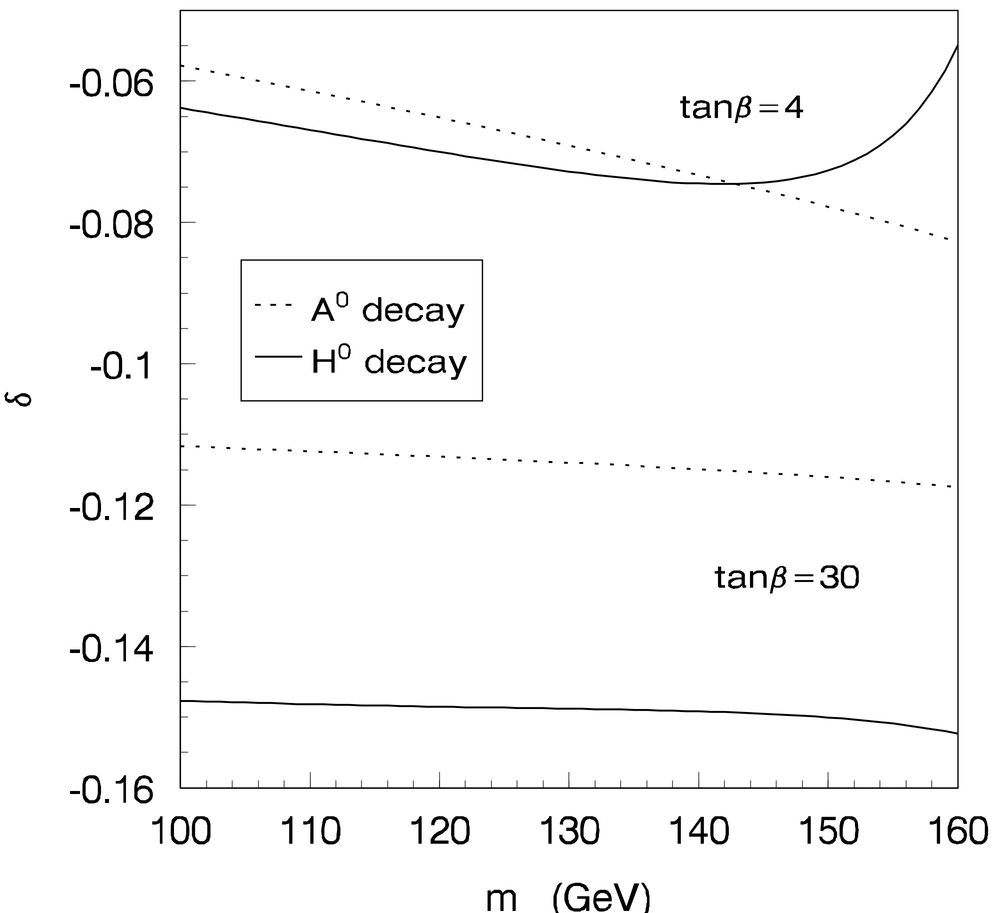
-0.06
-0.08
-0.1
-0.12
-0.14
-0.16
δ
100
110
120
130
140
150
160
$m_{\chi_1^+}$(GeV)
tanβ = 4
tanβ = 30
A⁰ decay
H⁰ decay

Fig.9

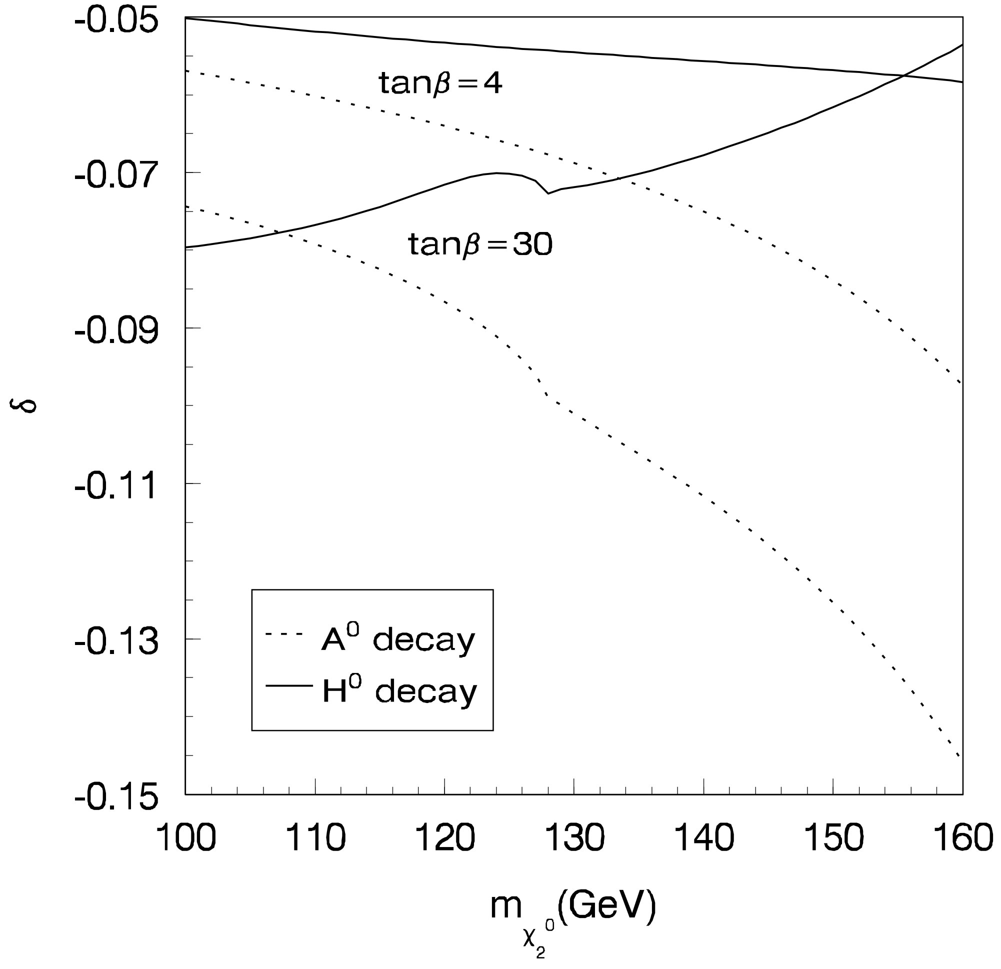

-0.05
-0.07
-0.09
-0.11
-0.13
-0.15
δ
100
110
120
130
140
150
160
$m_{\chi_2^0}$(GeV)
tanβ = 4
tanβ = 30
A^0 decay
H^0 decay